FORCE-DEFLECTION CHARACTERIZATION OF INDIVIDUAL CARBON NANOTUBES ATTACHED TO MEMS DEVICES

[1]A. B. Hartman, [2]P. Rice, [1,2]D. S. Finch, [3]G. D. Skidmore, and [1]V. M. Bright
[1]University of Colorado at Boulder, Department of Mechanical Engineering
Colorado, USA
[2]National Institute of Standards and Technology
Colorado, USA
[3]Zyvex Corporation
Texas, USA

ABSTRACT

Results are presented for in-situ manipulation, attachment, and mechanical testing of individual carbon nanotubes (CNTs) on MEMS devices. Nanotubes positioned onto polysilicon structures were permanently attached by electron beam deposition (EBD) "welding". This approach allows design of mechanical tests for nanotubes with commercially available MEMS processes. A tensile force of 2.4 +/- 0.2 μN was applied to the structure via an attached, individual CNT, producing device deflections measured in a scanning electron microscope. Based on atomic force microscopy of welds, the joint between the EBD material and MEMS surface supported a shear stress of 1.6 +/- 0.5 MPa.

1. INTRODUCTION

Background

The mechanical, thermal, and electrical properties of carbon nanotubes (CNTs) make them desirable components in micro/nano systems. Application as high aspect ratio atomic force microscope (AFM) tips [1], wires in nano-electronics [2], and shafts for nano-gears [3] has been proposed. However, CNT properties must first be characterized before they can be implemented as engineering structures.

Previous work has shown directed growth of many freestanding nanotubes on surfaces [4]. Other research has deposited CNTs onto a substrate and fabricated suspended, torsional "paddle" devices on top of single tubes using standard thin-film deposition techniques [5]. An alternative approach used electron beam deposition (EBD) and in-situ manipulation, permitting study of the electrical conductivity for individual tubes as they were mechanically stressed [6]. Further work demonstrated similar manipulation techniques to integrate a CNT onto a MEMS device designed to measure the tube's electrical response to tensile loading [7].

2. EXPERIMENTAL

Approach

In this work we have used a pick-and-place strategy, inside a scanning electron microscope (SEM), to investigate CNT mechanical properties. As a first step, we have concentrated on measuring force-deflection curves for individual CNTs mounted on MEMS platforms. Nanotubes previously prepared on glass slides have been manipulated to the desired device site, permanently attached, pulled, and the resulting device deflections measured.

Nanotube Preparation

For manipulation, it was vital that the free end of a tube be accessible. Surfactant coated, multi-walled CNTs in de-ionized water were received from the Grulke group at the University of Kentucky [8]. Samples were rinsed and stored in high purity methanol to remove this coating. To provide free ends, a small drop of the CNT suspension was first deposited onto a glass slide and the liquid allowed to evaporate, leaving a mat of CNTs behind. A second, gold-coated glass slide was pulled over a piece of SEM carbon tape, forming a thin layer of adhesive on the gold at the edge of the slide. This adhesive layer was then dragged across the dried tubes. Large bundles from the mat were adhered to the adhesive, such that free ends of the CNTs were found to extend well past the edge of the glass. This CNT-bearing slide was finally mounted in the SEM, gold side up, with silver loaded epoxy or carbon tape used to reduce charging of the slide and CNT bundles.

Manipulation and Attachment

In order to position single CNTs at a chosen position on the MEMS device, a custom-built nanomanipulator was used. It utilized piezoelectric inchworm actuators to provide three degrees of freedom, X-Y-Z, with nanometer step sizes and 10 mm travel. The entire device was designed to fit inside the SEM chamber, and was equipped with a tungsten probe end effector.

Electron beam deposition inside SEMs was investigated as early as 1953 [9]. Organic materials present inside the chamber, such as vacuum pump lubricants and surface adsorbed grease, were dissociated by the electron beam. Carbon atoms freed in this way accumulated at the surface being imaged. By holding the beam in spot mode and dwelling at a particular location, this accumulation built up into an EBD "weld. A 3D AFM scan of a deposit formed at 10 kV accelerating voltage, 40 pA beam current, and a 10 minute dwell time, is given in Figure 1. For these

0-7803-8265-X/04/$17.00 ©2004 IEEE.

conditions, a typical deposit height and diameter were 0.6 μm and 1.5 μm, respectively.

EBD was used to weld a CNT to the probe tip. A typical pick and place sequence followed these steps: (a) the tungsten probe tip approached an exposed CNT, (b) a CNT was tacked to the tip with a short duration EBD weld, (c) the

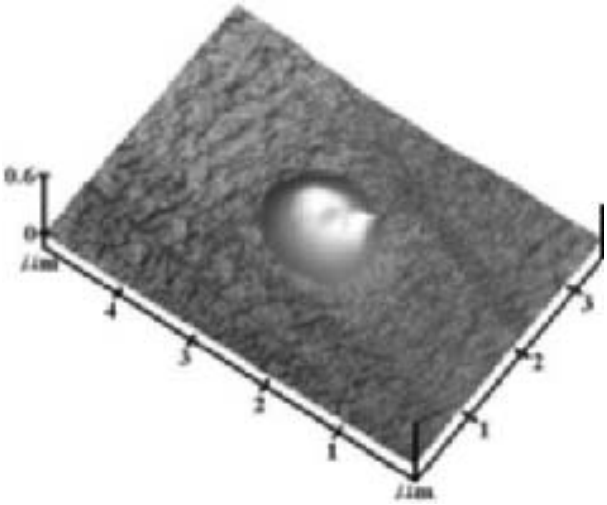

Figure 1: 3D AFM scan of EBD on a silicon surface. Height is approximately 0.6 μm.

probe was retracted, straightening the tube, (d) further retraction removed a single CNT from the bundle, (e) one CNT end was positioned on the device surface and permanently welded, and finally (f) the temporary weld to the probe was broken, and the other CNT end pressed onto the surface and welded. Figure 2 depicts each step in the process. The result was an individual CNT rigidly attached to two separate MEMS surfaces. Figure 3 shows an example of a CNT welded at both ends across a gap between two polysilicon structures.

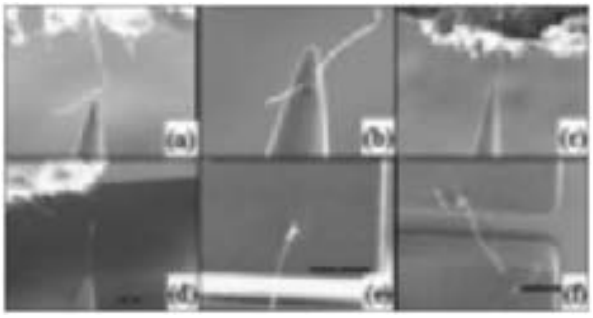

Figure 2: CNT manipulation procedure, showing (a-b) approach and interim weld, (c-d) extraction, and (e-f) full welds. CNT diameter approximately 100 nm in all images.

Measurement

Figure 4 shows a polysilicon [10] tensile test device designed to simultaneously measure applied force and elongation of an attached CNT. The welds and CNT were tested for their ability to withstand forces necessary to produce observable deflections of the gauge flexure. One end of a tube was welded to the flexure, and the other end to a tungsten probe. The probe pulled the tube and flexure, and digital image analysis was used to determine the deflections. Measurement of the flexure displacement to +/- 0.1 μm was achieved against the anchored metric provided near the gap between the actuator and flexure.

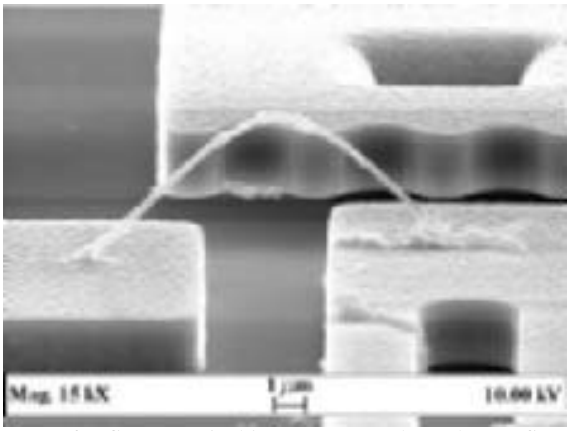

Figure 3: CNT attached between two released MEMS structures.

3. ANALYSIS

In order to know the force applied to the tube, a non-linear, finite element model was established to determine the force-deflection relationship for the gauge flexure. Static simulations were conducted in 2D using plane elements [11]. Similar 3D analyses using shell elements [11] and solid elements [12] verified that no deflections occurred out-of-plane, and that a 2D model was sufficient.

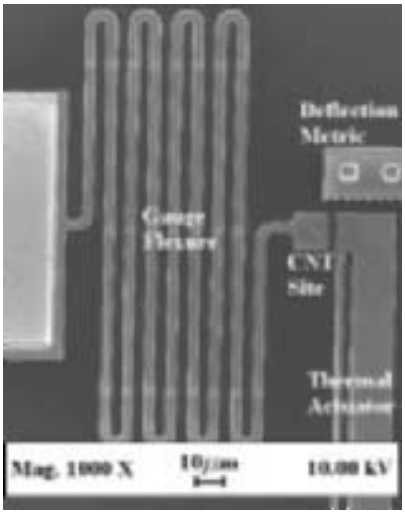

Figure 4: Tensile testing device for CNTs.

An analytical solution was also developed to validate the simulation results. The flexure geometry was broken into a

number of symmetric, U-shaped segments and treated as a collection of linear springs in series that, when connected head to tail, formed the meander shape. Castigliano's theory for bending was used to analyze one such segment. Equal and opposite forces were applied to the ends of the segment, perpendicular to the straight sections. The resulting relationship between deflection δ and load F was

$$\delta = \frac{F}{6EI}\left(4L^3 + 6L^2\pi R + 24LR^2 + 3\pi R^3\right),$$

with Young's modulus E, flexure cross-section moment of inertia I, length of a straight section for one segment L, and radius for the curved section of a segment R. For N similar segments the overall stiffness of the flexure design was

$$k = \frac{6EI}{N\left(4L^3 + 6\pi L^2 R + 24LR^2 + 3\pi R^3\right)}.$$

Figure 5 shows predictions from the finite element models and the analytical solution. Over a deflection range of 0.1-10 μm, both approaches agreed to within 0.6 %.

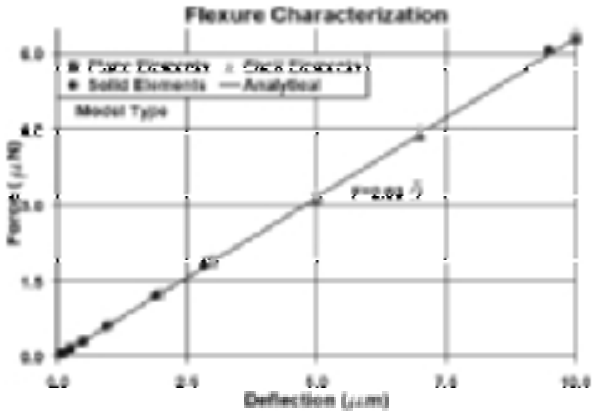

Figure 5: Comparison of models for spring constant of gauge flexure.

4. RESULTS

Data was analyzed using values summarized in Table 1. The flexure stiffness was found to be 0.63 +/- 0.06 μN/μm, based on uncertainty analysis.

Table 1: Dimensions for gauge flexure.

Variable	Value
N - Number of segments	8
L - Length	75 μm
R - Radius	4 μm
E - Young's modulus	169 GPa
I - Moment of inertia	10.7 μm^4
Cross-section base	2 μm
Cross-section height	4 μm

Figure 6 shows a series of SEM images taken with a CNT attached between a polysilicon flexure and a moving tungsten probe installed in the manipulator. The maximum deflection of the flexure was 3.8 +/- 0.1 μm. With this displacement, a calculated tensile force of 2.4 +/- 0.2 μN was applied to a MEMS structure via an attached, individual CNT. Based on AFM measurements of welds created under similar conditions, the diameter of the EBD weld was 1.4 +/- 0.2 μm. Assuming a rigid weld, and that the force in the CNT acts parallel to the flexure's top surface, the EBD-polysilicon interface supported a shear stress of 1.6 +/- 0.5 MPa.

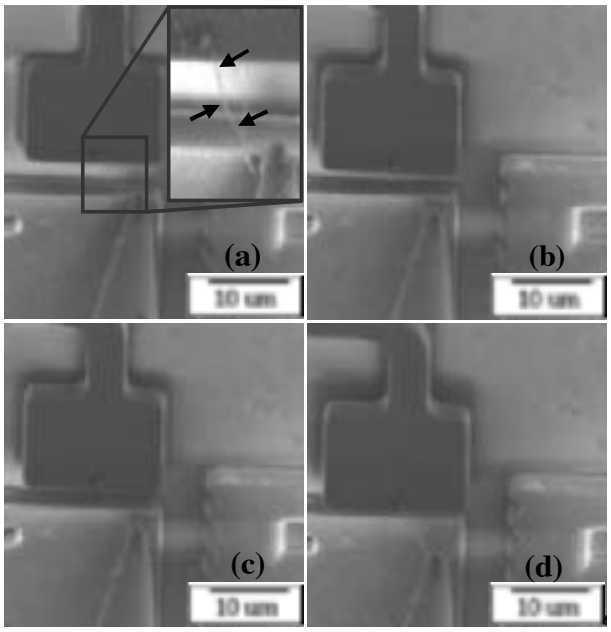

Figure 6: MEMS flexure deflected by attached CNT. (a) Starting position with inset highlighting tube. (b-d) Device movement caused by pulling probe.

In addition to testing with a tungsten probe, nanotubes were also connected between the actuator and flexure on four separate devices. The actuators were powered and observed under an optical microscope. Actuators could be seen to move approximately 4 μm and then stop, because of forces in the CNTs. Deflections of the flexure could not be resolved optically. It was not possible to determine whether this lack of observable deflection was due to stiction between the flexure and substrate, or insufficiently powerful actuators. It is interesting to note, however, that two devices were observed to have sudden, additional actuator deflections when powered beyond the stopping point, possibly indicating that the tube had failed under loading.

5. CONCLUSIONS

MEMS devices provide an excellent platform for testing of individual CNTs. By using an in-situ nanomanipulation scheme, it is possible to integrate single CNTs directly onto commercially fabricated MEMS devices. This allows researchers to rapidly create specific nanotube test. Also, the EBD welding process creates bonds to both nanotubes and

polysilicon that are strong enough to transfer loads capable of causing microns of displacement in MEMS structures.

Acknowledgements

The authors thank Prof. Martin Dunn, Dr. Nils Hoivik, Kimberly Tuck, and Neil Sarkar for their useful discussions about this work, and Dr. David Read for the use of the nanomanipulator. This research is supported by Zyvex Corporation, as part of the NSF Center for Advanced Manufacturing and Packaging of Microwave, Optical, and Digital Electronics (CAMPmode), University of Colorado.

REFERENCES

[1] H. Dai, J. Hafner, A. Rinzler, D. Colbert, R. Smalley, "Nanotubes as nanoprobes in scanning probe microscopy", *Nature*, vol. 384, pp. 147-149, 1996.

[2] S. Tans, M. Devoret, H. dai, A. Thess, R. Smalley, L. Geerligs, C. Dekker, "Individual single-wall carbon nanotubes as quantum wires", *Nature,* vol. 386, pp. 474-477, 1997.

[3] J. Han, A. Globus, R. Jaffe, G. Deardorff, "Molecular dynamics simulations of carbon nanotube-based gears", *Nanotechnology*, vol. 8, pp. 95-102, 1997.

[4] A. Cassell, N. Franklin, T. Tombler, E. chan, J. Han, H, Dai, "Directed growth of free-standing single-walled carbon nanotubes", *J. Am. Chem. Soc.,* vol. 121, pp. 7975-7976, 1999.

[5] P. Williams, S. Papadakis, A. Patel, M. Falvo, S. Washburn, R. Superfine, "Torsional response and stiffening of individual multiwalled carbon nanotubes", *Phys. Rev. Letters,* vol. 89, no. 25, article 255502, 2002.

[6] M. Yu, M. Dyer, G. Skidmore, H. Rohrs, XK. Lue, K. Ausman, J. von Her, R. Ruoff, "Three-dimensional manipulation of carbon nanotubes under a scanning electron microscope", *Nanotechnology,* vol. 10, pp. 244-252, 1999.

[7] P. Williams, S. Papadakis, M. Falvo, M. Sinclair, A. Seeger, A. Helser, R. Taylor II, S. Washburn, R. Superfine, "Controlled placement of an individual carbon nanotube on a microelectromechanical structure", *Appl. Phys. Letters*, vol. 80, pp. 2574-2576, 2002.

[8] http://www.mrsec.uky.edu/direct/grulke.htm

[9] A. Ennos, "The origin of specimen contamination in the electron microscope", *Br. J. of Appl. Phys.,* vol. 4, no. 4, pp. 101-106, 1953.

[10] http://www.memscap.com/memsrus/crmumps.html

[11] http://www.ansys.com

[12] http://www.coventor.com